12

Instability and Turbulence

Instability is of interest largely because it creates turbulence. But the relationship between instability and turbulence is complex. To take advantage of the relative simplicity of linear instability theory, we must understand that relationship much better than we do today.

One approach is to relax the assumption of small-amplitude perturbations by numerically solving the fully nonlinear equations. This reveals a sequence of instabilities that lead to turbulence (section 12.1).

Though we think of instability as the "cause" of turbulence, that causality can actually be reversed. In section 12.2 we will explore two mechanisms by which turbulence can create instability.

In observational science, we find that nature rarely cooperates in creating the simple, idealized scenarios that our equations and theorems can describe. Instead, we must take a step back and look at turbulence from a less-rigorous, yet intuitively appealing, perspective such as that described in section 12.3.

12.1 Secondary Instabilities and the Transition to Turbulence

What happens after an unstable mode begins to grow? At some point it becomes large enough that our linearized equations become invalid. Exponential growth is damped. Beyond this time, the disturbance may simply decay, or it may exhibit a secondary instability. Analysis of this evolution is extremely difficult, and is best done using a direct numerical simulation (DNS) of the fully nonlinear equations of motion.

12.1.1 Nonlinear Development

Figure 12.1 shows a sequence of snapshots from DNS of a stratified shear layer. Initially, the minimum Richardson number is 0.08, so the Miles-Howard instability

https://doi.org/10.1017/9781108640084.013 Published online by Cambridge University Press

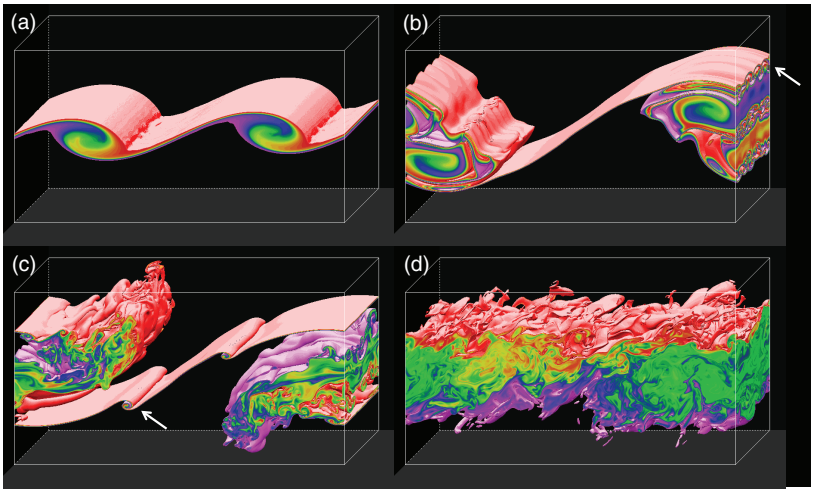

Figure 12.1 Snapshots of the buoyancy field from a nonlinear simulation of an unstable shear layer as it becomes turbulent. (a) Kelvin-Helmholtz instability. (b) Subharmonic pairing instability, convective instability (arrow). (c) Secondary Kelvin-Helmholtz instability (arrow). (d) Turbulence. Parameter values $Ri_b = 0.08$, $Re = 800$, $Pr = 7$. Horizontal boundaries are periodic. Colors range from $-0.6b_0$ to $+0.6b_0$; values outside this range are transparent. (Smyth and Thorpe, 2012)

criterion is easily satisfied. The horizontal boundaries are periodic, with domain length chosen to accommodate two wavelengths of the fastest-growing mode.[1] In the first snapshot (Figure 12.1a), the fastest-growing mode has grown to form a sequence of billows (compare with Figure 4.4, for example). Within each billow is a region where dense fluid overlies buoyant fluid, inviting convective instability.

The next stage is the growth of a subharmonic instability, which causes adjacent billows to pair. The result appears as a single large billow straddling the edge of the domain (Figure 12.1b). This instability is essentially a manifestation of the primary instability with wavenumber equal to half that of the fastest-growing

[1] The molecular properties of the modeled fluid are consistent with thermally inhomogeneous water. The kinematic viscosity ν is $1.0 \times 10^{-6}\mathrm{m^2 s^{-1}}$ and the diffusivity κ is $1.4 \times 10^{-7}\mathrm{m^2 s^{-1}}$, so that the Prandtl number is 7. Domain dimensions are $4.19 \times 0.87 \times 2.18$ m. The domain is designed to accommodate two wavelengths of the primary Kelvin-Helmholtz instability and four of the secondary convective instability. Boundary conditions are periodic in the horizontal directions, and free-slip and insulating in the vertical. Initial mean profiles of streamwise velocity and density are chosen to represent a stratified shear layer:

$$\frac{U(z)}{u_0} = -\frac{B(z)}{b_0} = \tanh\frac{z}{h}$$

with half-changes $b_0 = 1.6 \times 10^{-5}$ m s^{-2} in buoyancy and $u_0 = 5.3 \times 10^{-3}$m s^{-1} in velocity, and half-thickness $h = 0.15$ m. A small perturbation is added to excite primary and secondary instabilities. The minimum Richardson number is Ri_b is 0.08 and the initial Reynolds number Re is 800.

https://doi.org/10.1017/9781108640084.013 Published online by Cambridge University Press

mode. Although its growth rate is relatively small, its large wavelength allows it to grow more or less independently of the fastest-growing mode, and when it reaches large amplitude it simply swallows up the original billows. If Ri is small enough, this process can occur repeatedly as successively larger modes reach finite amplitude. This is an example of an upscale energy cascade, in which kinetic energy is transferred to successively larger-scale motions.

Within the merging billows, we see a row of four convection cells resulting from the convective overturning noted earlier (arrow on figure 12.1b). Note that the cells are oriented in the direction of the mean flow, as predicted by stability theory (homework problem 19, Appendix A). This secondary instability grows very quickly, leading to the development of turbulence within the core of the merged billow (Figure 12.1c).

In the center of the domain, the strain between the large billows compresses the transition layer to form a sharp gradient of buoyancy and velocity. If the gradient Richardson number in that thin layer is small enough, secondary Kelvin-Helmholtz billows develop. The secondary convective and Kelvin-Helmholtz instabilities are examples of a downscale energy cascade, in which energy is transferred to successively smaller motions. The ultimate result of the cascade is that the entire structure breaks down into turbulence (Figure 12.1d).

This is only one possible evolution of a stratified shear layer. With different values of Ri_b, Re, and Pr, different sequences of secondary instabilities are found. In nature, billows often bypass the subharmonic pairing instability and break down directly into smaller-scale motions.

12.1.2 Return to Stability

Instability can be thought of as the means by which an unstable flow adjusts to a stable state. In Figure 12.1d, for example, the transition layer is much thicker than it was initially (Figure 12.1a). If we take horizontal averages of velocity and buoyancy and compute the bulk Richardson number, it ends up greater than its initial value by a similar factor (Figure 12.2). That final value is greater than the critical value 1/4. In other words, the end state consists of a *stable* stratified shear layer plus decaying turbulence. This state of gradual decay persists indefinitely, unless some external force re-accelerates the shear layer. That possibility is the subject of section 12.3.

12.2 Turbulence-Driven Instabilities

In contrast to instability causing turbulence, we now look at two cases where turbulence causes instability.

https://doi.org/10.1017/9781108640084.013 Published online by Cambridge University Press

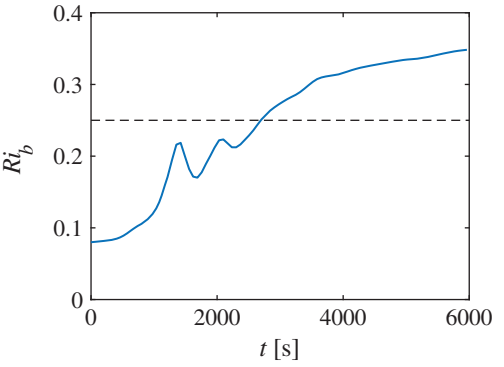

Figure 12.2 Evolution of the bulk Richardson number in the DNS shown in Figure 12.1.

12.2.1 Phillips' Layering Instability

While molecular viscosity and diffusivity can usually be regarded as constant, turbulent viscosity and diffusivity vary in space and time. Because viscosity and diffusivity change in response to changes in the flow, there is a potential for positive feedback and hence instability.

Consider a highly idealized fluid in which

- buoyancy $b(z, t)$ varies with height and (possibly) time, and
- the only motion is in the form of small-scale turbulence, which alters b via a turbulent diffusivity $K(z, t)$.

The evolution of b is governed by the diffusion equation:

$$\frac{\partial b}{\partial t} = -\frac{\partial F}{\partial z}.$$

where F is the vertical buoyancy flux due to turbulence:

$$F = -K\frac{\partial b}{\partial z}.$$

Differentiating with respect to z yields an equation for the buoyancy gradient b_z:

$$\frac{\partial b_z}{\partial t} = \frac{\partial^2}{\partial z^2}(Kb_z), \tag{12.1}$$

where the subscript z indicates the partial derivative, just like $\partial/\partial z$.

Now suppose that the turbulent diffusivity K is determined by b_z, so that $K = K(b_z)$. For example, it is plausible to think that turbulence would be weaker in strongly stratified regions, in which case K would be a decreasing function of

https://doi.org/10.1017/9781108640084.013 Published online by Cambridge University Press

b_z. This creates the possibility of a positive feedback between stratification and turbulence.

Imagine now that b_z consists of a constant plus a small perturbation:

$$b_z = b_{z0} + b_z'(z,t),$$

and approximate $K(b_z)$ by a first-order Taylor series expansion

$$K = K_0 + K^* b_z',$$

where the constant K^* is defined as

$$K^* = \left(\frac{\partial K}{\partial b_z}\right)_{b_z = b_{z0}}. \tag{12.2}$$

If, as we have imagined, turbulence is reduced in regions of stronger stratification, then $K^* < 0$.

We now write the buoyancy flux as

$$F = -Kb_z = -(K_0 + K^* b_z')(b_{z0} + b_z') = -K_0 b_{z0} - K_0 b_z' - b_{z0} K^* b_z'.$$

The quadratic term has been neglected as usual. Substituting this into (12.1), we have

$$\frac{\partial b_z'}{\partial t} = \frac{\partial^2}{\partial z^2}\left[K_0 b_{z0} + (K_0 + b_{z0}K^*) b_z'\right] = (K_0 + b_{z0}K^*)\frac{\partial^2 b_z'}{\partial z^2}.$$

The perturbation b_z' is therefore governed by a standard diffusion equation in which the "diffusivity" is $K_0 + b_{z0}K^*$. If K^* is not only negative but less than $-K_0/b_{z0}$, then this effective diffusivity is negative. Buoyancy gradients, rather than being smoothed over time, become sharper.[2] Negative diffusivity can lead to the formation of layers of uniform buoyancy ($b_z = 0$) separated by thin layers in which buoyancy changes rapidly. Step-like features observed in the ocean (e.g., Figure 12.3) may be accounted for by instabilities like this.

12.2.2 Thermohaline Interleaving

Steppy profiles of temperature and salinity like those shown in Figures 9.10 and 9.11 are ubiquitous in the ocean. Here we'll look at a second possible explanation for these features. In the previous section we supposed that the buoyancy flux between adjacent layers was carried by some generic brand of turbulence. A slightly more complicated variant of this instability involves gradients of both temperature and salinity and fluxes driven by turbulent salt fingering (section 9.2.4). As

[2] This is like the diffusion of money: the rich get richer, and the poor get poorer.

https://doi.org/10.1017/9781108640084.013 Published online by Cambridge University Press

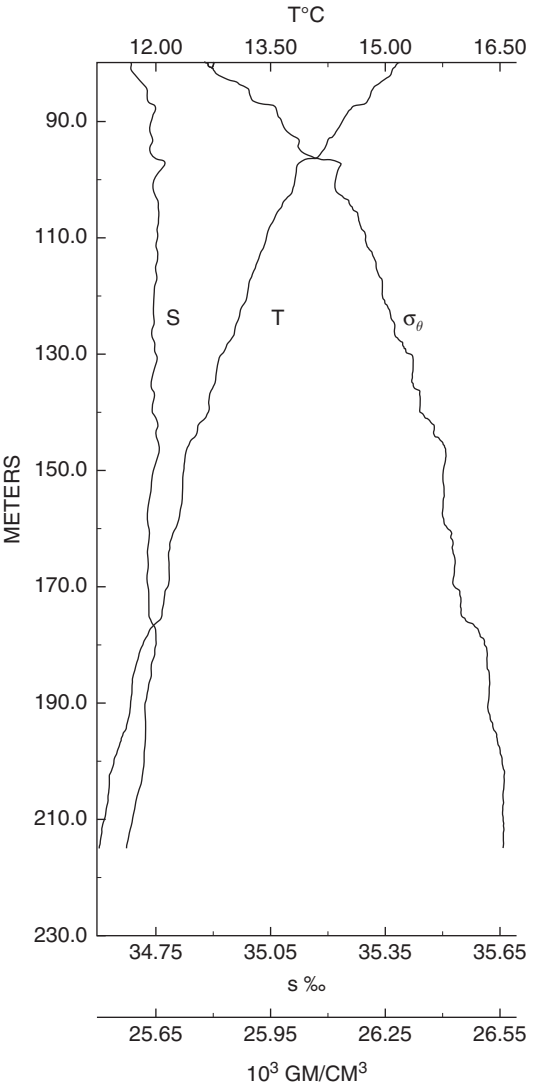

Figure 12.3 Profiles of salinity, temperature, and density measured in the California current (Gregg, 1975). Salinity S is in parts per thousand by mass, temperature T is in degree Celsius. Density is represented as σ_θ = potential density minus 1000 kg/m^3.

salt fingers grow, they eventually break down and become turbulent, but they continue to carry with them an upward flux of buoyancy. As in the previous subsection, variations in that buoyancy flux can create a new instability.

Imagine a fluid stratified by both temperature and salinity so that warm, salty water overlies cool, fresh water, the configuration suitable for salt fingering

https://doi.org/10.1017/9781108640084.013 Published online by Cambridge University Press

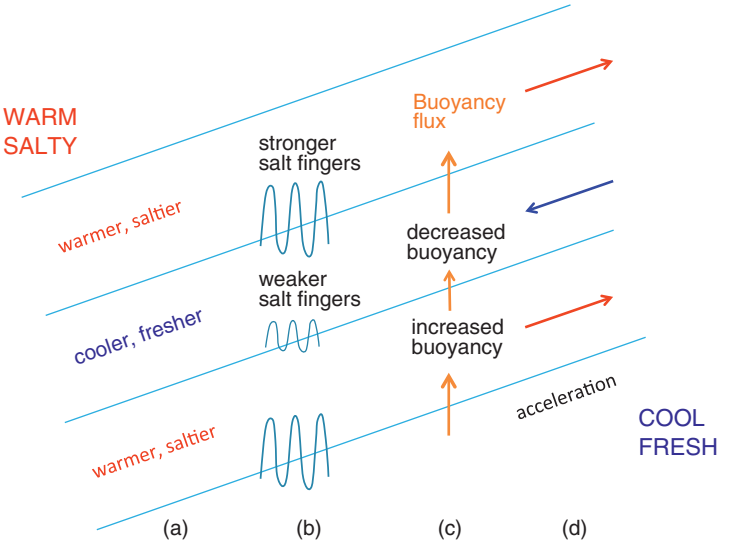

Figure 12.4 Schematic of thermohaline interleaving instability. Overall stratification favors salt fingering, i.e., warm, salty fluid over cool, fresh fluid, but the gradients also have a horizontal component. Temperature and salinity perturbations (a) have the form of tilted layers. At the layer boundaries, perturbations alternately enhance and diminish the tendency to form salt fingers (b), along with the upward buoyancy flux the fingers carry (c). As a result, alternating layers become more and less buoyant, causing them to slide (d). This motion advects the temperature and buoyancy fields so as to increase the perturbations.

instability (section 9.2.4). Imagine further that the temperature and salinity gradients both tilt upward to the left as shown in Figure 12.4. For simplicity, we will also assume that the temperature and salinity gradients balance exactly so that the density is the same everywhere.

Now imagine a normal mode disturbance that induces in-phase perturbations of temperature and salinity on tilted layers as shown. In between two such layers, the stratification becomes either slightly more favorable to salt fingering, or slightly less so. Like all convective motions, salt fingers carry an upward buoyancy flux, and that flux is stronger when the salt fingering is stronger.

As a result of the varying buoyancy flux, alternating layers become lighter and denser, so that gravity pulls them upward to the right or downward to the left. These motions advect the original temperature and salinity gradients so as to reinforce the perturbation. This positive feedback leads to exponential growth of the disturbance.

Interleaving is common wherever currents of water with different properties meet. For example, warm, salty water from the North Atlantic flows into the cold, fresh Arctic Ocean through Fram Strait (Figure 12.5, red and green curves). The purple curve shows inflow from the Barents Sea, where the temperature/salinity

https://doi.org/10.1017/9781108640084.013 Published online by Cambridge University Press

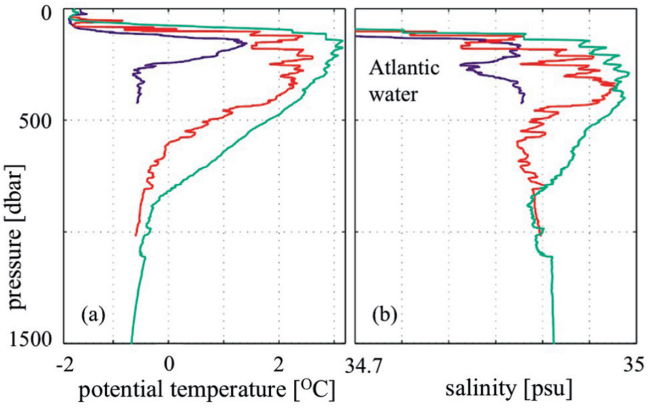

Figure 12.5 Potential temperature (a) and salinity (b) profiles from the eastern Kara Sea slope. Pressure [dbar] is equivalent to depth in meters. Red and green curves show Atlantic water interleaving with Arctic water. Adapted from Rudels et al. (2009).

contrast is reduced and interleaving is less prominent. Interleaving layers in the Arctic are the largest in the world ocean, extending over ∼1000 km.

Interleaving can also be driven by diffusive convection (section 9.2.5). In Figure 12.5, interleaving on the upper (lower) edge of the Atlantic layer is driven by diffusive convection (salt fingering). Shear instability can develop on the boundaries between the oppositely moving layers. If the temperature and salinity gradients do not exactly balance, the resulting lateral density gradient can be balanced by the Coriolis force as in Chapter 8 so that the motion takes on some aspects of baroclinic instability.

12.3 Cyclic Instability

In instability theory, we assume that at some initial time the flow takes a very simple, laminar, equilibrium form. The equilibrium is then perturbed, and we compute the initial growth of the perturbation. In real geophysical fluids this specific chain of events is rare. Instabilities observed in nature grow in environments that are already turbulent, thanks to previous instabilities. At large amplitude, instabilities break and generate turbulence whose ultimate effect is to return the mean flow to a stable state.

The hypothesis of cyclic instability suggests that a flow can remain in a state of approximate equilibrium through the combined action of external forcing, which tends to destabilize the flow, and sporadic instabilities, which restore stability. A nice analogy was proposed by Bak et al. (1987): a sandpile is continually steepened by the addition of more sand, but if it becomes too steep, an avalanche will form, reducing the slope to a stable value (Figure 12.6). Through the action of many,

https://doi.org/10.1017/9781108640084.013 Published online by Cambridge University Press

Figure 12.6 A marginally stable, forced-dissipative system. The angle of repose is maintained, on average, by random, small avalanches. Source: iStock/Getty Images

sporadic avalanches, the slope is maintained, on average, at the *angle of repose*. That angle depends on the grade of the sand.

Called self-organized criticality in the physics community, this behavior is characteristic of many forced-dissipative systems. Other examples include earthquakes, forest fires, and solar flares (Aschwanden, 2016). In the case of geophysical turbulence, we imagine that some external force such as the wind acts continually to destabilize the fluid while sporadic turbulent events relieve the instability.

Figure 12.7 shows an example from the eastern equatorial Pacific Ocean. The trade winds blow the surface water to the west, generating the south equatorial current (SEC, Figure 12.7a). These pile up against the Asian coastlines, and the weight of that extra water increases the subsurface pressure. The resulting pressure gradient drives a return flow at around 100 m depth, the equatorial undercurrent (EUC). Shear and stratification both increase to maxima just above the EUC core (Figure 12.7b). Their ratio, Ri (Figure 12.7c), is remarkably uniform over much of this depth range, and is conspicuously close to Miles and Howard's critical value 1/4 (section 4.7). We'll have more to say about this shortly.

A useful measure of turbulence intensity is the rate at which turbulent kinetic energy is dissipated by viscosity, ϵ.[3] In our example from the EUC, turbulence remains strong down to 80 m depth (Figure 12.7d). Because this turbulence coexists with strong stratification, the turbulence is doing a lot of work against gravity by exchanging warm, buoyant water from the surface mixed layer with cold water from the thermocline. This is one reason that the eastern equatorial Pacific is the global maximum of ocean heat uptake.

Now as for the Richardson number being "conspicuously close" to 1/4, what is happening (Figure 12.8) is that forcing from the trade winds acts continuously to increase the shear, and therefore to decrease Ri. But whenever Ri drops below

[3] Equation (5.35) gives the linearized form.

https://doi.org/10.1017/9781108640084.013 Published online by Cambridge University Press

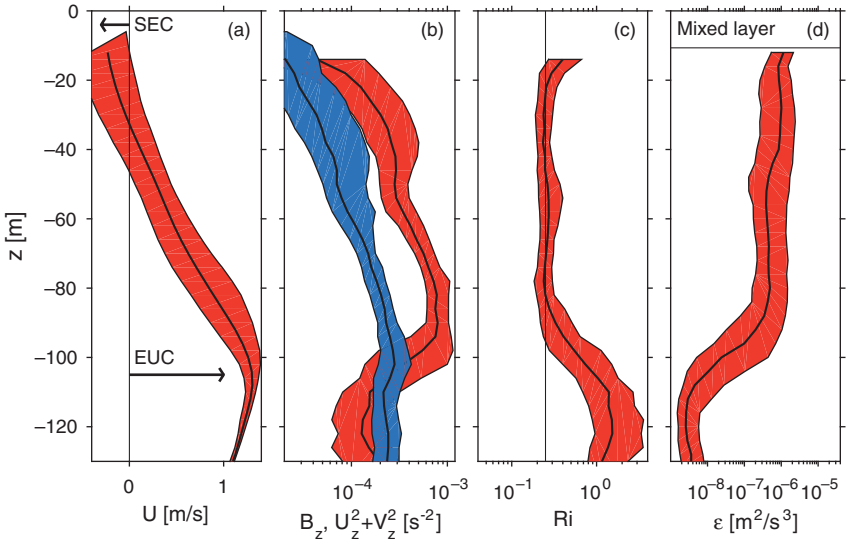

Figure 12.7 Mean flow and turbulence in the upper equatorial Pacific. Two weeks of shipboard observations were taken on the equator at 140 W in October, 2008. Profiles show the median and the quartile range at each depth. (a) Zonal velocity, showing the South Equatorial Current and the Equatorial Undercurrent. (b) Buoyancy gradient B_z (blue) and squared shear (red). (c) Gradient Richardson number with the vertical line at $Ri = 1/4$. (d) Turbulent kinetic energy dissipation rate. See Smyth and Moum (2013) for further details.

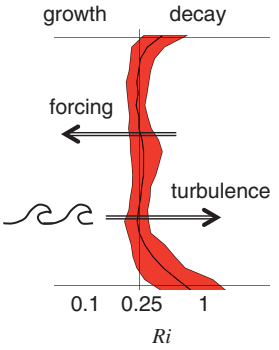

Figure 12.8 Schematic of cyclic instability. The red area shows a Richardson number profile from the upper equatorial Pacific (cf. Figure 12.7c).

1/4, instability generates turbulence, which mixes out the shear, thereby increasing Ri to values greater than 1/4 (as in section 12.1.2). The ultimate result is that Ri fluctuates more or less randomly around 1/4.

https://doi.org/10.1017/9781108640084.013 Published online by Cambridge University Press

This is the oceanic analog of the sandpile described earlier. The trade winds correspond to the sand source and sporadic shear instabilities to the avalanches. The "angle of repose" for stratified turbulence is the critical state $Ri = 1/4$.

12.4 Further Reading

- The original discussion of self-induced criticality is Bak et al. (1987). Comprehensive overviews may be found in Jensen (1998) and Aschwanden (2016).
- The sequence of secondary instabilities that leads a Kelvin-Helmholtz billow train to the turbulent state is described in Mashayek and Peltier (2012a,b).
- Posmentier (1977) provides a nice explanation of the layering instability.
- For more information on thermohaline interleaving, try Ruddick and Kerr (2003), Ruddick and Richards (2003), Smyth and Ruddick (2010), or Radko (2013).
- For more on marginally unstable states and cyclic instability, see Thorpe and Liu (2009), Smyth and Moum (2013), or Smyth et al. (2017).